Songklanakarin J. Sci. Technol.
32 (3), 289-297, May - Jun. 2010

Songklanakarin Journal of Science and Technology
http://www.sjst.psu.ac.th

Original Article

Improvement on design analyses of composite steel-concrete bridges using elaborate finite element methods

Jaturong Sa-nguanmanasak[1]*, Taweep Chaisomphob[1] and Eiki Yamaguchi[2]

[1] *School of Civil Engineering and Technology, Sirindhorn International Institute of Technology, Thammasat University, Khlong Luang, Pathum Thani, 12121 Thailand*

[2] *Department of Civil Engineering, Kyushu Institute of Technology, Tobata, Kitakyushu 804-8550, Japan*

Received ; Accepted

Abstract

In this paper, three-dimensional finite element analysis of composite steel-concrete bridges is performed to simulate the actual bridge behavior. The accuracy of the model is verified against the results acquired from a field test. Thai trucks are loaded at possible locations of the bridge in order to obtain the maximum stresses on the bridge. The influences of concrete barriers, the displacement of bridge piers, and the Young's modulus of concrete are then discussed, to reveal the actual behavior of the steel-concrete composite bridge. The reactions at the bearings on the bridge piers are also evaluated and discussed in this conjunction. Good agreement is obtained between the models and loading tests to show that the finite element model can aid engineers in design practices.

Keywords: composite, finite element, barrier, pier, field test.

1. Introduction

A traffic jam is a very serious problem in many major cities in Southeast Asia. Bangkok in Thailand is one of those cities that have suffered the problem for many years. To alleviate it, the Bangkok Metropolitan Administration conducted a project of constructing overpasses at busy junctions recently. Fast construction was an essential requirement since the construction site was inevitably in the area of heavy traffic. To this end, a standard design of an overpass was set up, and the project was completed in about two years.

Those overpasses are steel-concrete composite bridges made of steel plate I-girders, concrete decks, and steel bridge piers. The employment of the steel girders and the steel piers is to decrease the dead loads of the overpasses, helping to reduce the size of foundation and to shorten the construction period. Upon completion, Rama III–Sathu Pradit Bridge, one of the overpasses in the project, was tested by static truck loads to confirm the performance.

In this paper, the structural behavior of a steel-concrete composite bridge is studied. In particular, Rama III–Sathu Pradit Bridge (Figure 1) is selected, since it is a typical

Figure 1. Rama III–Sathu Pradit Bridge.

* Corresponding author.
Email address: jaturong@siit.tu.ac.th

example of the built overpasses and in-situ measurements under the known loads are available.

The finite element method has been used to simulate successfully the behavior of a bridge in the past. Three dimensional nonlinear finite element models are generated to predict the actual behavior of masonry arch bridges (Fanning and Boothby, 2001). The dynamic characteristics of the cable-stayed bridge are studied by three-dimensional finite element models (Zhang *et al.*, 2001). The stress analysis of a long-span cable stayed bridge from finite element analysis compared very well with a full-scale static loading test (Lertsima *et al.*, 2004). The dynamic interaction between a heavy truck and highway is presented by the finite element analysis (Kwasniewski *et al.*, 2006). Three-dimensional nonlinear finite element analysis of two-plate-girder bridge is conducted to obtain dry shrinkage and prestressing (Yamaguchi *et al.*, 2005). The finite element method in combination with the boundary element is applied to analyze box-girder bridges (Galuta and Cheung, 1995). Finite element models are examined to predict the stress and deflection of steel-concrete composite girders (El-Lobody and Lam, 2003; Chung and Sotelino, 2006). Dynamic finite element modeling of composite girder-slab bridge provided approximations of the dynamic properties (Farrar and Duffey, 1998). The structure behavior of bridge deck slabs under static patch loads in steel-concrete composite bridges has been studied by using a non-linear 3D-finite element analysis models with ABAQUS software (Zheng *et al.*, 2009). The non-linear finite element models have been applied for single-arch bridges, the new Svinesund Bridge, link between Norway and Sweden. Multi-response objective function are introduced, which allow the combination of static and dynamic measurements to obtain a solid basis for parameter estimation (Schlune *et al.*, 2009).

In the present study, the discrepancy between the design values and the test results is examined by conducting a finite element analysis, based on which the factors responsible for the structural behavior of the steel-concrete composite bridge are discussed. The finite element program, MARC (1994) is used in this study.

2. Rama III–Sathu Pradit Bridge

Rama III–Sathu Pradit Bridge consists of 13 spans, as its schematics are shown in Figure 2(a). Each span is simply supported on steel bridge piers. The span length where the loading test was conducted is 31.5 m and the structural information on this part of the bridge is given in Figure 2 and Table 1.

The superstructure is a steel-concrete composite bridge with two traffic lanes. It has four steel I-girders of 1.45 m height with the space of 2.1 m in-between and a concrete deck of 200 mm thickness connected to the girders by studs. The bridge piers are steel structures, consisting of a column and a partly-double beam. The design is based on AASHTO Standard Specifications for Highway Bridges (1996).

Each steel girder has two bearings, one on Pier S6 and the other on Pier S7. All the translational movements relative to the beam of the bridge pier are constrained at the bearings on Pier S7 while only the vertical movement relative to the beam of the bridge pier is constrained at the bearings on Pier S6. No rotational degrees-of-freedom are constrained at all the bearings.

Since the bridge has four girders, each pier has four bearings on it. Out of the four bearings, two are located on the

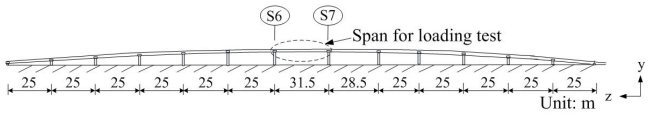

(a) Side view.

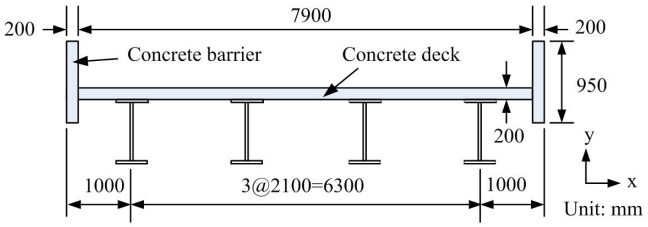

(b) Cross section of the superstructure.

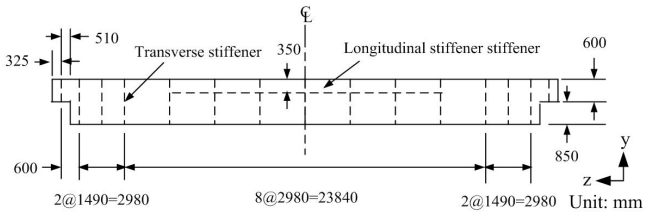

(c) Side view of steel girder.

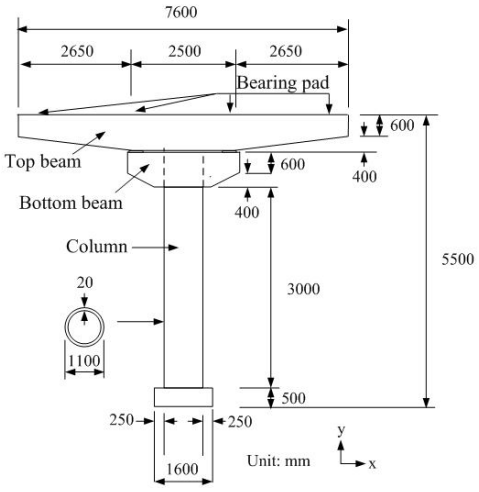

(d) Bridge pier.

Figure 2. Rama III–Sathu Pradit Bridge.

Table 1. Dimensions of cross section.

(a) Main girder

	Main girder	Cross girder stiffener	Transverse stiffener	Longitudinal
Bu (mm)	300(300)	199	-	-
tu (mm)	13(13)	11	-	-
Hw (mm)	1450(600)	374	120(140)	120
tw (mm)	9(9)	7	9(15)	9
Bl (mm)	400(400)	199	-	-
tl (mm)	20(20)	11	-	-
A (cm^2)	249.5(173)	72.16	10.8(21)	10.8
I_x (cm^4)	$8.33\times10^5(1.20\times10^5)$	$2.00x10^4$	0.73(3.94)	0.73
I_y (cm^4)	$1.36\times10^4(1.36\times10^4)$	$1.45x10^3$	$1.30\times10^2(3.43\times10^2)$	1.30×10^2

( ): End girder

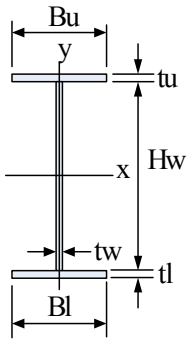

Main girder/Cross girder

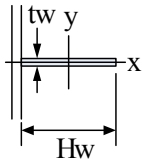

Vertical stiffener/Longitudinal stiffener

(b) Cross frame

	Top girder	Bottom girder	Diagonal member
B (mm)	80	80	75
tf (mm)	11	11	9
Hw (mm)	200	200	75
tw (mm)	7.5	7.5	9
A (cm^2)	31.33	31.33	12.69
I_x (cm^4)	$1.95 x10^3$	$1.95 x10^3$	64.4
I_y (cm^4)	$1.68x10^2$	$1.68x10^2$	64.4

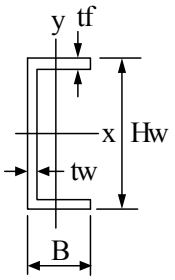

Top girder/bottom girder

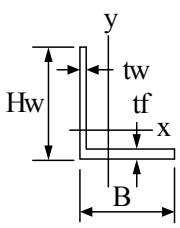

Diagonal member

(c) Pier

	Top beam	Bottom beam	Column	
			Main part	Bottom part
Bu (mm)	1300	1300	1100	1100
tu (mm)	13	15	20	20
Hw (mm)	1000 (636)	604	-	-
tw (mm)	13	15	-	15
Bl (mm)	1300	1300	-	1600
tl (mm)	13	15	-	-
A (cm^2)	598 (503.36)	571.2	678.58	1728.58
I_x (cm^4)	1.08×10^6 (4.12×10^5)	4.29×10^5	2.47×10^8	1.54×10^9
I_y (cm^4)	1.18×10^6 (9.21×10^5)	9.20×10^5	1.29×10^9	7.66×10^9

( ): End girder

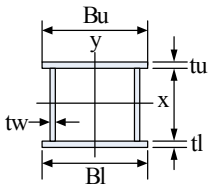

Top beam/Bottom beam

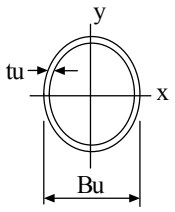

Column (Main part)

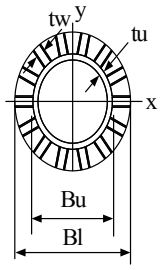

Column (Bottom part)

double-beam portion while the remaining two are on the single-beam portion.

Following the design of this bridge, Young's moduli of steel and concrete of this steel-concrete composite bridge may be assumed 206,000 N/mm^2 and 23,600 N/mm^2, respectively, and the Poisson's ratios of steel and concrete, 0.3 and 0.2, respectively.

3. Loading test

Three trucks, each weighs about 240 kN, are used for the loading test on Rama III–Sathu Pradit Bridge. The loading condition can be realized from the positions of the trucks shown in Figure 3. The axle loads are given in Figure 3(a). It is noted that a half of the wheels are located right above the web of Girder G4, which is one of the worst loading conditions for this external girder. Under this loading condition, the longitudinal normal strain and the vertical displacement of each lower flange of the four girders were measured at the mid-span: four values of the normal stress in the z-direction and four values of the displacement in the y-direction are therefore available.

4. Bridge models

As is often the case with design practices, only the superstructure consisting of a concrete deck and steel I-girders is considered first as a basic model and called Model 1; the influence of the displacements of the bridge piers are ignored. The finite element model is constructed with 13,112 8-node solid elements and 16,689 4-node shell elements. The solid elements are employed for the concrete deck, and the shell elements for steel girders and the cross frames.

The superstructure has a concrete barrier on each side. Although the contribution of the barriers to the structural stiffness is neglected in the design analysis, it is not necessarily negligible in reality. This aspect is to be studied herein. To this end, the concrete barriers are modeled by 4,520 8-node solid elements and are added to Model 1. This is called Model 2. The Young's modulus of the concrete barriers is assumed to be the same as that of the concrete deck, i.e. 23,600 N/mm^2.

Neglecting the displacements of the bridge piers, the movements of the bearings due to the deformation of the bridge piers are not taken into account in Model 1 and 2, which is a common practice in the design analysis. However, since the bridge piers are not rigid and can undergo deformation, the movements of the bearings may take place and influence the behavior of the bridge in reality. To investigate this point, the finite element models of the bridge piers are constructed and added to Model 2, which is Model 3 in this study. 10,510 4-node shell elements are used for each bridge

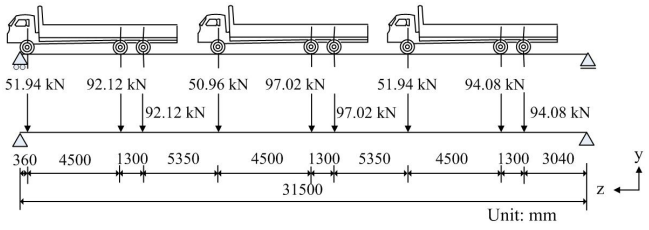

(a) Axle positions and magnitudes of axle loads.

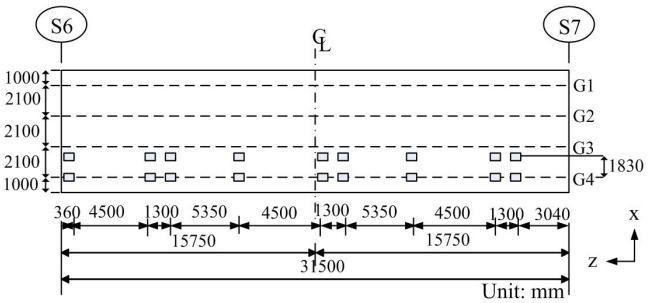

(b) Wheel positions.

Figure 3. Loading condition for three-truck loading test.

pier.

The control of the material properties of concrete is not easy and the variation of Young's modulus of concrete is inevitable. Nevertheless, the concrete with the design value of the Young's modulus of 23,600 N/mm^2 can be expected to have the value in the range of 20,000-30,000 N/mm^2 in Thai practice. To take into account this variation, Model 4-7 are prepared, each of which has a different combination of Young's moduli of concrete for the deck and the barriers (Table 2). The finite element discretizations for Model 4-7 are the same as that of Model 3. The finite element models are presented in Figure 4.

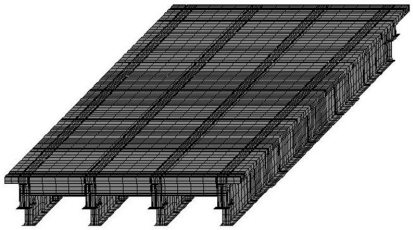

(a) Model 1.

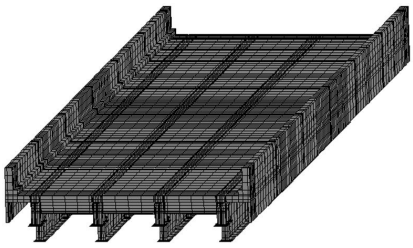

(b) Model 2.

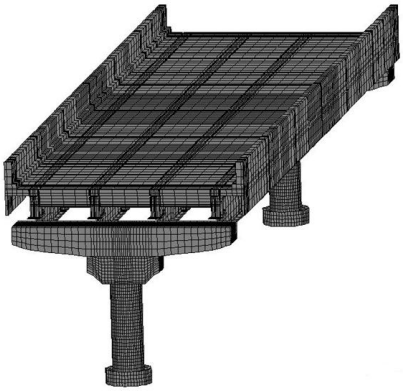

(c) Models 3-7.

Figure 4. Finite element models.

Table 2. Analysis models.

	Young's modulus (N/mm^2)		Interaction with piers
	Concrete deck	Concrete barrier	
Model 1	23,600	N	N
Model 2	23,600	23,600	N
Model 3	23,600	23,600	C
Model 4	23,600	20,000	C
Model 5	20,000	23,600	C
Model 6	23,600	30,000	C
Model 7	30,000	23,600	C

C: considered in the model; N: not considered in the model

5. Numerical results and Discussions

5.1 Influence of Concrete Barriers

The results by the finite element analysis (FEA) using Model 1 and 2 are shown in Table 3 and Figure 5 together with the loading-test results and the design values. It is observed that the design analysis tends to overestimate the stress and the vertical displacement measured in the loading test. The differences at the mid-span of Girder G4 are as much as 20.5 N/mm^2 or 58% in the stress and 6 mm or 25% in the vertical displacement. FEA by Model 1 also overestimates the stress measured in the loading test, but the difference is smaller than that due to the design analysis.

The inclusion of the concrete barriers in the analysis, i.e. FEA by Model 2, improves the stress significantly, yielding the stress values close to the stress measured in the loading test. On the other hand, the displacements obtained by Model 1 are better than those by Model 2. The loading test has shown large differences in the vertical displacement between Girders G4 and G1. Girder G1 moved even upwards in the test. However, Model 2 predicts much smaller differences in the vertical displacement between Girders G4 and G1, and the movement of Girder G1 is downward, which does not agree with the loading-test result.

Table 3. Stress and displacement at the mid-span.

(a) Normal stress (N/mm^2)

	G4	G3	G2	G1
Test	35.2	28.7	12.1	2.7
Design	55.7	43.0	24.3	3.7
Model 1	48.6	32.3	14.7	2.1
Model 2	38.8	27.3	13.5	1.2
Model 3	39.4	26.5	12.8	1.8
Model 4	40.3	26.9	13.0	1.7
Model 5	39.7	26.5	12.7	1.6
Model 6	38.0	25.7	12.5	2.0
Model 7	38.8	26.4	13.0	2.1

(b) Vertical displacement (mm)

	G4	G3	G2	G1
Test	-24	-15	-6	5
Design	-30	-23	-13	-2
Model 1	-24	-15	-7	1
Model 2	-17	-12	-6	-1
Model 3	-26	-16	-6	4
Model 4	-26	-16	-6	4
Model 5	-26	-16	-6	4
Model 6	-25	-15	-6	4
Model 7	-25	-15	-6	4

The trends in the present FEA are inconsistent: Model 2 gives better stress while Model 1 gives better vertical displacement. Because stress is closely related to deformation, it may be stated that Model 2 has simulated the deformation of the superstructure better. Considering that the girders of this bridge are statically determinate, the displacements at the bearings due to the deformations of the piers, if any, might change the deflection of the superstructure in the way of rigid-body movement, i.e. without much influencing the deformation of the superstructure, which may account for the inconsistency observed herein.

In any case, the results by Model 1 and 2 suggest the importance of the contribution of the concrete barriers to the actual structural behavior of this steel-composite bridge, as the two models yield quite different results.

5.2 Interaction between Superstructure and Bridge Pier

The results of FEA by Model 3 are presented in Table 3 and Figure 6. The stress values are not much different from those by Model 2, and they remain in good agreement with the test results. On the other hand, the vertical displacements

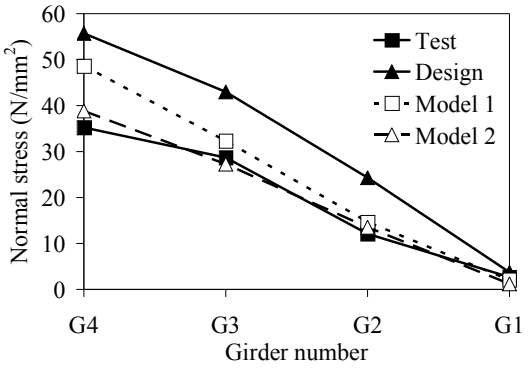

(a) Normal stress at the mid-span.

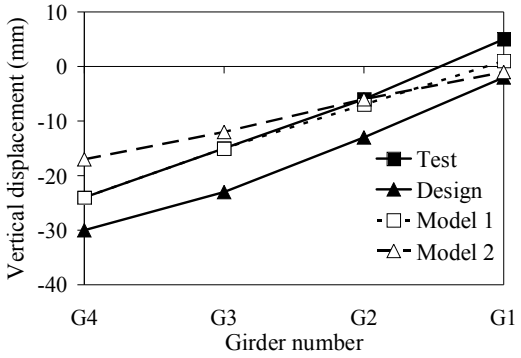

(b) Vertical displacement at the mid-span.

Figure 5. Influence of barriers on normal stress and vertical displacement.

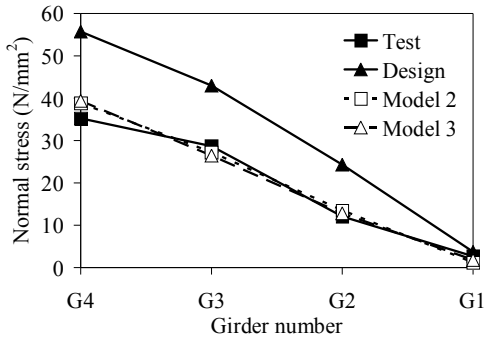

(a) Normal stress at the mid-span.

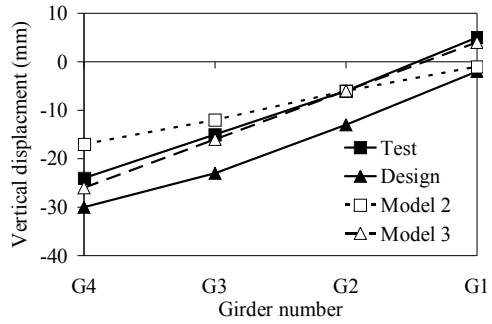

(b) Vertical displacement at the mid-span.

Figure 6. Influence of the interaction between superstructure and bridge Pier.

are noticeably improved by Model 3. In fact, the vertical displacements due to Model 3 compare very well with those measured in the loading test.

Table 4 shows the vertical displacements of the beams of the bridge pier at the bearings obtained in the analysis by Model 3. This data confirms that the bridge piers indeed deform and the beams of the bridge piers displace, which is not considered in the design analysis, though.

The amounts of the vertical displacements at Pier S6 and Pier S7 are similar to each other. The vertical displacements at the bearings are close to the differences in the mid-span vertical displacement between Model 2 and 3. As discussed previously at the end of Section 5.1, the displacements at the bearings may not change the stress states, even though they change the vertical displacements. This is exactly what seems to happen when the bridge piers are included in the finite element analysis, suggesting the importance of the inclusion of the bridge piers in the analysis to capture the actual structural behavior of an overpass. It should be noted that the deformations of the bridge piers are even more important if a bridge is continuous, i.e. statically indeterminate, since the stress states of the girders could be affected also by the vertical displacements of the beams of the bridge piers.

Table 4. Vertical displacement at the bearings (mm).

	G4	G3	G2	G1
S6	-8.3	-5.1	-0.4	5.3
S7	-8.2	-4.8	-0.2	5.1

5.3 Influence of Young's Modulus of Concrete

The influence of the variation of Young's modulus of concrete is studied by conducting FEA by Model 4 to 7. The results are presented in Table 3 and in Figure 7 together with those by Model 3. The Young's modulus of concrete is certainly influencing the structural behavior of the bridge, but the differences in the stress and the vertical displacement turn out to be very small. Therefore, it may be stated that the variation of Young's modulus of concrete is negligible for evaluating the structural behavior of a steel-concrete composite bridge.

5.4 Reactions at Bearings

The internal forces acting at the bearings between the superstructure and the bridge piers are called reactions herein. Those acting on the superstructure in Model 1 to 3

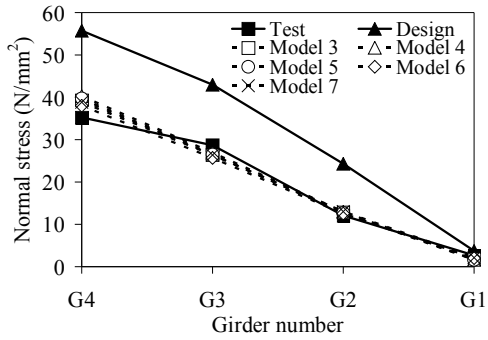

(a) Normal stress at the mid-span.

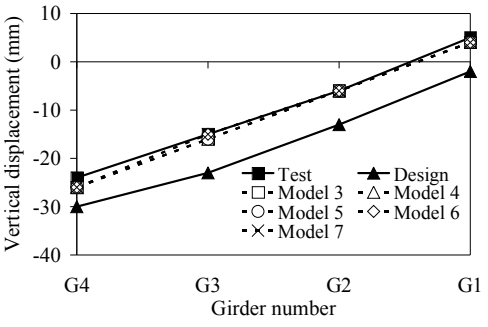

(b) Vertical displacement at the mid-span.

Figure 7. Influence of Young's modulus of concrete on normal stress and vertical displacement.

Table 5. Reactions (kN).

(a) S6 (y-direction)

Model	G4	G3	G2	G1
1	209.1	128.9	48.7	-22.5
2	225.0	103.2	52.4	-16.4
3	274.7	40.5	29.1	19.9

(b) S7

Model	G4			G3			G2			G1		
	x	y	z	x	y	z	x	y	z	x	y	z
1	-1.4	206.6	-0.7	-0.9	126.1	9.4	0.1	45.5	-16.8	2.2	-20.4	8.1
2	5.6	221.1	6.9	-2.3	102.3	-2.6	-3.8	49.9	-15.7	0.5	-15.4	11.3
3	2.9	245.6	26.3	-32.0	69.4	-31.8	25.5	41.5	-15.2	3.7	1.3	20.8

are summarized in Table 5. Very different results are obtained between the models.

Firstly, it is noted that the reactions in the y-direction at the bearings of Girder G1 in Model 1 and 2 are negative while the reaction in Model 3 is positive. The phenomenon can be accounted for as follows:

The loading condition in the present study is eccentric since all the truck loads are applied near Girder G4. This loading condition tends to move Girder G4 downward while Girder G1 tends to move upward. This causes the negative vertical reaction at the bearings of Girder G1 in Models 1 and 2, since the girders cannot move upward at the bearings. On the other hand, in Model 3 where the deformation of the bridge piers are also taken into account, the beams of the bridge piers displace, pushing up Girder G1, resulting in the positive vertical reactions at the bearings of Girder G1 in this model.

The differences in the other reactions between the three models are also noticeable. The inclusion of the concrete barriers and the bridge piers in the analysis is thus important for evaluating the reactions as well. To be noted, the negligence of these factors can yield smaller reactions at some bearings. The observation herein therefore implies that the design of the bearings can be not only wrong but also unsafe if the whole bridge is not modeled appropriately.

The present bridge is simply-supported. Therefore, no horizontal reactions need to be computed in the design. This is because each girder is assumed to deform independently in the design, once external loads are distributed to the girders. However, the assumption of the independent behavior of the girders is not true since the girders do interact through concrete deck and cross frames. The present results confirm the point, showing the existence of the horizontal reactions. The negligence of the horizontal loads in the design of the bearings therefore can be completely wrong. Caution must be used for the design of the bearings.

6. Conclusing Remarks

The structural behavior of a steel-concrete composite bridge, Rama III–Sathu Pradit Bridge located in Bangkok, is investigated. The following observations have been made in this study.

1. The design analysis consistently overestimates the longitudinal stress and the vertical displacement measured in the loading test. The differences at the mid-span of Girder G4, where the largest values were obtained, are as much as 20.5 N/mm^2 or 58% in the stress and 6 mm or 25% in the vertical displacements.

2. Although in the design analysis concrete barriers are treated as non-structural members and thus the contribution to the structural behavior of the bridge is ignored, they are indeed influencing the structural behavior. This fact partly accounts for the discrepancy of the design values from the loading-test results.

3. The interaction between the superstructure and the bridge piers is neglected in the design analysis. However, the bridge piers actually deform and influence the structural behavior of the bridge. The interaction may be even more important if a bridge is continuous, i.e. a statically indeterminate structure.

4. The influence of the variation of the Young's modulus of concrete on the structural behavior of a steel-concrete composite bridge is very small and may be neglected in the design analysis.

5. The finite element analysis can simulate the structural behavior of a steel-concrete composite bridge very well: the results would be in good agreement with those of loading test, provided that a finite element model takes account of all the contributing factors such as concrete barriers and bridge piers.

6. The real reactions can be quite different from those obtained in the design analysis. Not only magnitude but also

the directions of those forces can be different. Moreover, the horizontal reactions, which are neglected in the design analysis of a simply-supported girder, are present. Caution must be used for the design of the bearings.

7. The inclusion of the concrete barriers and the bridge piers in the analysis is important in the evaluation of reactions, since the negligence of these factors can yield smaller reactions. Therefore, the design of the bearings may be not only wrong but also unsafe if the whole bridge is not modeled appropriately.

8. For further study, more complicated three-dimensional finite element modeling should be investigated, for example, modeling of bearing pad included, and more details of pier foundation. Also, the application of a proposed model to various types of composite bridges should be explored, such as curved bridges, high-strength concrete/ prestressed concrete bridges.

Acknowledgements

The present research was partially supported by the Thailand Research Fund through the Royal Golden Jubilee Ph.D. Program (Grant No. PHD/0028/2544). It is also the outgrowth of the academic agreement between Sirindhorn International Institute of Technology, Thammasat University, and the Faculty of Engineering, Kyushu Institute of Technology, and has been partially supported by the two academic bodies. These supports are gratefully acknowledged. The authors are also grateful to Bangkok Metropolitan Administration and Unique Engineering and Construction Public Co. Ltd. for their supports in the full-scale loading test of the Rama III–Sathu Pradit Bridge.

References

AASHTO. 1996. LRFD Bridge Design Specifications, First Edition, American Association of State Highway and Transportation Officials, Washington, DC.

Chung, W. and Sotelino, E.D. 2006. Three-dimensional finite element modeling of composite girder bridges, Engineering Structures. 28(1), 63-71.

El-Lobody, E. and Lam, D. 2003. Finite element analysis of steel-concrete composite girders, Advances in Structural Engineering. 6(4), 267-281.

Farrar, C.R. and Duffey, T.A. 1998. Bridge modal properties using simplified finite element analysis, Journal of Bridge Engineering, ASCE. 3(1), 38-46.

Fanning, P.J. and Boothby, T.E. 2001. Three-dimensional modeling and full-scale testing of stone arch bridges, Computers and Structures. 79(29), 2645-2662.

Galuta, E.M. and Cheung, M.S. 1995. Combined boundary element and finite element analysis of composite box girder bridges, Computers and Structures. 57(3), 427-437.

Kwasniewski, L. Li, H. Wekezer, J. and Malachocwski, J. 2006. Finite element analysis of vehicle-bridge interaction, Finite Element in Analysis and Design. 42(11), 950-959.

Lertsima, C. Chaisomphob, T. and Yamaguchi, E. 2004. Three-dimensional finite element modeling of a long-span cable bridge for local stress analysis, Structural Engineering and Mechanics. 18(1), 113-124.

MARC Analysis Research Corporation. 1994. MARC Manuals-Vol. A-D, Rev. K.6, Palo Alto, Calif.

Schlune, H. Plos, M. and Gylltoft, K. 2009. Improved bridge eveluation through finite element model updating using static and dynamic measurements, Engineering Structures. 31(7), 1477-1485.

Yamaguchi, E. Fukushi, F. Hirayama, N. Kubo, T. and Kubo, Y. 2005. Numerical study of stress states near construction joint in two-plate-girder bridge with cast-in-place PC slab, Structural Engineering and Mechanics. 19(2), 173-184.

Zhang, Q.W. Chang, T.Y.P. and Chang, C.C. 2001. Finite-element model updating for the Kap Shui Mun cable-stayed bridge, Journal of Bridge Engineering, ASCE. 6(4), 285-293.

Zheng, Y. Robinson, D. Taylor, S. and Cleland D. 2009. Finite element investigation of the structural behaviour of deck slabs in composite bridges, Engineering Structures. 31(8), 1762-1776.